Cement & Concrete Composites 30 (2008) 815–821

Contents lists available at ScienceDirect

Cement & Concrete Composites

journal homepage: www.elsevier.com/locate/cemconcomp

Sulphate resistance of lime-based barium mortars

Ioannis Karatasios [a,*], Vassilis Kilikoglou [a], Panagiotis Theoulakis [b], Belinda Colston [c], David Watt [d]

[a] Institute of Materials Science, NCSR Demokritos, Aghia Paraskevi, Athens 153 10, Greece
[b] Department of Conservation of Antiquities and Works of Art, TEI of Athens, Athens 122 10, Greece
[c] Department of Forensic and Biomedical Sciences, University of Lincoln, Lincoln LN6 7TS, UK
[d] Hutton and Rostron Environmental Investigations Limited/Centre for Sustainable Heritage, University College London, UK

ARTICLE INFO

Article history:
Received 12 September 2007
Received in revised form 23 June 2008
Accepted 24 June 2008
Available online 2 July 2008

Keywords:
Restoration mortars
Lime
Barium hydroxide
Acid attack
Sulphates
Conservation

ABSTRACT

This work studies the effect of barium hydroxide on the sulphate-resistance of lime-based mortars when used as an additive material to the lime binder. The overall aim of the work is to study the potential of barium hydroxide in producing a mixed binder with lime, which is able to fix the sulphate ions, block the diffusion of sulphate solutions and therefore, reduce the degradation rate of mixtures.

The durability of different mixtures was studied through sulphate salt crystallisation and acid rain simulation tests, along with the characterisation of their pore-space properties. X-ray diffraction (XRD), scanning electron microscopy (SEM/EDX) and inductively coupled plasma-atomic emission spectroscopy (ICP-AES) were used for materials characterisation. Experimental results proved that barium hydroxide increases the durability of hardened mixtures against sulphate attack, without affecting the microstructure characteristics.

1. Introduction

Lime-based mortars have been widely used in archaeological and historic monuments for both decoration and protection purposes (renders, facades, etc.). Over past decades, the degradation rate of mortars exposed to urban environments has increased due to the impact of environmental pollution on building materials [1,2], affecting their performance characteristics, as well as the amenity of historic buildings. The degradation of lime mortars also has economic consequences as the total damage cost, which is the sum of the renovation cost and the amenity loss, increases. In this context, the understanding of the degradation mechanisms of traditional mortars, and the development of new restoration mortars with enhanced durability, is of great importance and has been the subject of several projects [3–8].

The main process related to the degradation of mortars in an urban atmosphere is the reaction of the binding material with sulphate, either in the gaseous form (SO_x) or liquid phase (sulphuric acid) [1,3,6]. Sulphuric acid (H_2SO_4) readily reacts with calcite ($CaCO_3$) to form gypsum ($CaSO_4 \cdot 2H_2O$) through the mechanism of wet or dry deposition. In static conditions (humid air), the precipitation and nucleation of gypsum on the calcitic surface is favoured, and because of their greater solubility, surface gypsum layers exposed to rain are gradually washed out, increasing the porosity of the affected areas [9,10]. Weathering experiments have shown that the above transformation is rapid, and that gypsum formation can occur within a few days under normal atmospheric conditions [11,12].

In the case of cement mortars, or when other hydraulic binders are present, ettringite ($3CaO \cdot Al_2O_3 \cdot 3CaSO_4 \cdot 32H_2O$) and thaumasite ($CaSiO_3 \cdot CaCO_3 \cdot CaSO_4 \cdot 15H_2O$) are the two main products, which are formed through the sulphation process. Both products are highly expansive, and hence their formation leads gradually to the total destruction of the material [13–16].

Besides urban environments, ground water may also contain soluble sulphates from the extended use of chemicals in agriculture over past decades. As a consequence, the long-term service life of mortars, either buried, or in contact with ground water, can be affected [17].

The main factor controlling the resistance of mortars against sulphate attack is the chemistry of their binder [18]. A typical approach for reducing the degradation rate of restoration mortars involves the partial replacement of lime with pozzolanic materials. Pozzolans modify both the chemical properties of the binder and the pore-space characteristics of the mixtures, and therefore affect the long-term durability of mixtures exposed to sulphate environments [19–23].

Aiming to enhance the durability of restoration mortars against sulphate attack, this paper investigates the effect of barium hydroxide on the chemical resistance of lime-based mixtures, when it is used as an additive material to the lime binder. Previous

* Corresponding author. Tel.: +30 210 6503326; fax: +30 210 6519430.
E-mail address: ikarat@ims.demokritos.gr (I. Karatasios).

0958-9465/$ - see front matter © 2008 Elsevier Ltd. All rights reserved.
doi:10.1016/j.cemconcomp.2008.06.010

work on the setting process of lime-based barium mixtures revealed that barium hydroxide may be mixed with lime putty to create a homogeneous binder. This binder sets through the carbonation of both calcium hydroxide and barium hydroxide, the precipitation of calcite ($CaCO_3$) and witherite ($BaCO_3$), as well as the formation of a barium–calcium carbonate [$BaCa(CO_3)_2$] solid solution [24]. The formation of this solid solution results in the chemical compatibility of barium hydroxide with the lime binder and, through the spontaneous fixation of sulphate by barium carbonate, creates a potential shield against the chemical degradation of the binding material of lime-based mortars.

The present paper examines the effect of barium hydroxide on the chemical durability of new mixtures, as well as its effect on the pore-space properties and the movement of water solutions in the above mortars. This information is of great importance for studying the potential of barium hydroxide to produce a mixed binder capable of fixing sulphate ions, blocking the diffusion of sulphate solutions and, therefore, reducing the degradation rate of mortars used for restoration purposes. The overall aim of the work presented is to produce new mixtures for restoration purposes, compatible with traditional lime mortars, with enhanced sulphate resistance.

2. Experimental

In order to assess the relative resistance of different barium mixtures against sulphate attack, a number of accelerated aging laboratory tests were carried out. The aim of these tests was to determine the effect of barium hydroxide on the durability of the mixtures and to identify the parameters and the conditions for optimum performance. Prior to the accelerated aging tests, the mineralogical composition and the microstructural properties of mixtures were determined.

2.1. Test specimens

The test specimens were composed of lime putty, barium hydroxide, aggregates and water. The binder to aggregate ratio was set at 1:3 by volume. The aggregate fraction consisted of equal parts of calcitic sand and ceramic fragments in the range of 0.125–2.00 mm. The grain-size distribution chosen was based on the recommendations proposed by the BS EN 196-1 standard [25]. The density of lime putty was 1400 kg/m^3, barium hydroxide was 1360 kg/m^3 and the ceramic aggregates was 2350 kg/m^3. Barium hydroxide was added to the mixtures (BaM-10, BaM-25) in the solid state in two different amounts, constituting 10% and 25%, respectively, of the total binder volume of the reference mixture (LM–R). Previous work on barium–calcium hydroxide binary pastes has shown that the concentration of $Ba(OH)_2$ should not exceed 25% for optimum performance [24]. Finally, the water to binder ratio was set at 0.55 for all mixtures, according to the results of the flow test values.

The specimens were initially stored at a relative humidity of 90 ± 5%, and 20 ± 2 °C air temperature, for 7 days, followed by a period of 28 days at a relative humidity of 65 ± 5% (20 ± 2 °C). After this period, the specimens were removed from the moulds, placed on a thick plastic grid and stored in the laboratory room until testing, at a temperature of 20 ± 2 °C and a relative humidity of 50 ± 5% [25].

2.2. Setting products

Mineralogical analysis of mortar mixtures, cured for 12 months, was carried out by X-ray powder diffraction (XRD) before any other experimental process was carried out. Powder samples were drilled from a layer of 10–15 mm thick. X-ray diffraction analysis was performed on a Siemens D-500 Diffractometer using the Cu–K_α radiation (λ = 1.5406 Å) with a graphite monochromator in the diffraction beam, at 1.2 kW (40 kV, 30 mA). Spectra were collected in the range of 2–60° 2θ, with a step of 0.03°/s.

2.3. Pore-space properties

The formation of pore structure in the mortar mixtures is of great importance as it has a direct influence on the absorption, movement and evaporation of aqueous solutions through the mortar mass [26,27]. The efficiency of different types of mortar to absorb water is described through the determination of the water absorption coefficient (C) and water vapour permeability. Water vapour permeability values of mortars describe the ability of different types of mixtures to permit the diffusion and evaporation of water vapours and/or other water solutions through their mass, under isothermal conditions. This, in turn, controls a number of setting and deterioration mechanisms, such as carbonation, dissolution of binding material, salt crystallization and frost action.

The water absorption coefficient was measured in prism specimens, at atmospheric pressure, according to the test procedure described in BS EN 1015-18 and 1925 standards [28,29]. The base of the specimens was immersed in water to a depth of (3 ± 1) mm and the increase in their mass was measured as a function of time. Water vapour permeability determination was carried out according to the BS EN 1015-19 standard [30]. The specimens were sealed on the top of circular cups in which the water vapour pressure was maintained constant, at the upper part of the hygroscopic range, by means of potassium nitrate (KNO_3) saturated solution. The rate of the moisture transfer was determined by measuring the weight change of the cups. A graph of the mass of the cup was plotted against time and the water vapour flux ($\Delta G/\Delta t$) was calculated and the water vapour permeance (Λ) for each specimen was determined.

Finally, open porosity (p_o) of mixtures was determined by mercury intrusion porosimetry (MIP), in the range of 26–60,000 PSI. However, a considerable amount of the large pores, air voids and micro-cracks, which are formed during the setting of mortars could not be determined by mercury, as their dimensions exceeded the detection limits of the instrument. Therefore, in order to extend the measuring range from the μm to the mm scale, the open porosity values were also calculated by water absorption, according to the BS EN 1936 standard [31]. All properties were determined on mortar mixtures cured for 12 months.

2.4. Durability monitoring tests

2.4.1. Crystallisation by total immersion

This test simulated the potential deterioration mechanisms caused by the crystallisation of soluble salts under natural environmental conditions. The test consisted of monitoring the behaviour of mortars over time and assessing their relevant resistance against salt crystallisation. Accelerated aging was carried out by immersing mortar specimens in a 14% w/w sodium sulphate solution, according to the procedure described in BS EN 12370 [32]. The cycle of operation was repeated until the specimens collapsed. At the end of each cycle, the weight difference of the samples (ΔM) was calculated.

2.4.2. Acid attack

The aim of the acid attack test was to study chemical degradation caused by the dilute solutions of sulphuric acid in an attempt to simulate the deterioration of mortars exposed to external conditions due to acid rain. The test was focused on the dissolution of binder in the surface zone caused by an acidic solution. Since no

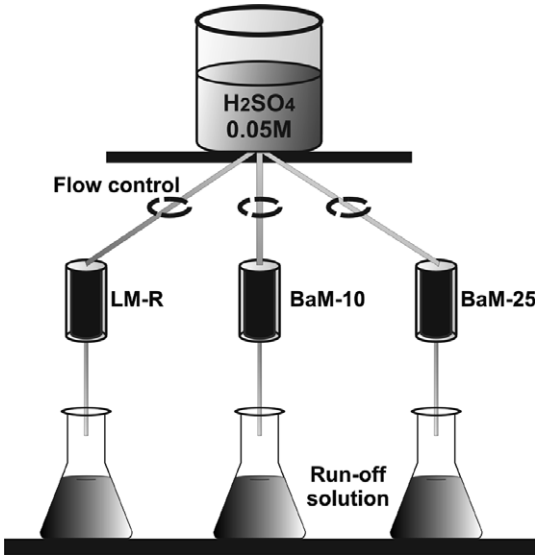

Fig. 1. Schematic diagram of the experimental set-up for simulating acid attack.

standard methodology exists for studying the chemical durability of mortars, an artificial weathering test was designed, based on previous work in the field [7,33]. Three cylindrical specimens from each mixture were placed in plastic tubes, allowing 1 mm free space around their surface. The solution was introduced at the top of the tube, flowing over the surface of the specimen and exiting at the bottom (Fig. 1).

The exposure protocol involved repeated cycles of exposure to a dilute solution of sulphuric acid (0.05 M, pH = 1.55) for 2 h, followed by drying at room temperature for 22 h. A solution flow rate of 0.5 L/h was employed, for an exposure period of 20 days. Prior to testing, the specimens were dried at 80 ± 5 °C until constant mass, and then allowed to cool at room temperature and weighed.

The run-off solutions were collected in conical flasks for chemical analysis. The accumulative elemental concentrations of calcium (Ca) and barium (Ba) were determined by inductively coupled plasma-atomic emission spectroscopy (ICP-AES) after 4, 12, 20 and 40 h of exposure, with the use of an Optima 3000 (Perkin Elmer, USA) unit. After the completion of the exposure time, the specimens were dried at 80 °C and weighed. Weight changes were determined in terms of percentage (%). Additionally, compositional and structural changes of mortars were determined by XRD and scanning electron microscope (JEOL 5310), respectively, coupled to an Oxford EDX analyser (SEM/EDX). The analysis was carried out using the INCA/ISIS microanalysis suite.

3. Results and discussion

3.1. Setting products

The main phases identified in the reference mixture (LM–R) were calcite ($CaCO_3$), portlandite [$Ca(OH)_2$] and a small amount of quartz. Calcite is produced by the carbonation of the lime binder, whilst portlandite is attributed to the non-carbonated lime putty. Calcite and witherite ($BaCO_3$) were the main products identified in the mixtures that contained barium hydroxide hydrate (BaM-10 and BaM-25), along with portlandite and some small amounts of quartz or clay minerals. X-ray diffraction analysis showed that barium–calcium carbonate [$BaCa(CO_3)_2$] was also formed within the binder of the above mixtures. The interaction between barium and calcium was also evident under the SEM. X-ray mapping showed that barium (Ba) was evenly distributed through the mortar mass, increasing its concentration around the calcite grains [24]. The formation of a barium–calcium carbonate offers a new matrix, which acts as a bridge between calcitic aggregates, barium phases and lime binder, contributing to the formation of a more homogeneous microstructure. This could be beneficial to the chemical durability of these mixtures.

Finally, examination of the mixtures under SEM verified that pozzolanic reactions had taken place between lime and the ceramic material, which resulted in the narrow formation of hydrated phases (C–S–H, C–A–H), with the typical needle-like shape.

3.2. Pore-space properties

The open porosity values of the reference mixture (32.90%) appeared to be very close to that of BaM-10 (32.79%), whereas BaM-25 appeared to have somewhat increased values (36.40%). However, the porosity values determined by water absorption gave a smaller range of values, between 36% and 37% (Table 1). The main differences between the open porosity values of the mixtures, determined by mercury intrusion porosimetry, fell within a range of 1000 and 10,000 nm pore radius (Fig. 2). In this range, the barium mixtures increased the amount of capillary pores from 200 cm^3/g (LM–R) to 275 cm^3/g (BaM-25). This has a slight effect on the transport properties of aqueous solutions and, therefore, the mixtures BaM-10 and BaM-25 have greater water absorption coefficients (kg/m^2), an increase of 14.8% and 16.6%, respectively (Table 1). In a similar manner, permeability values (kg/m^2 s Pa) were found to be elevated by 6.21% and 14.48%, for mixtures BaM-10 and BaM-25, respectively.

However, the above variations in the water absorption coefficient and the water vapour permeability values are not considered to be significant for the microstructure characteristics of the mixtures, since the pore-size distribution and the water accessible porosity values of all three mixtures remain the same. Therefore, all mixtures were considered to exhibit similar behaviour, reflecting a homogenous and similar microstructure.

3.3. Crystallisation of soluble salts

The first specimen to collapse during crystallisation tests was the reference mixture (LM–R) at the 7th aging cycle, followed by BaM-10 and BaM-25 at the 9th and 10th cycle, respectively. Freshly fractured surfaces of samples taken from the specimens during the crystallisation cycles were examined under a scanning electron microscope (SEM/EDX). The identification of the phases

Table 1
Mean values of open porosity, water absorption coefficient, rate of water absorption and water vapour permeability of the mixtures

Mixture	Open porosity (%)		Water vapour permeability (kg/m^2 s Pa) 10^{-11}	Water absorption coefficient C_1 (kg/m^2)	Rate of water absorption C_2 (g/m^2 $s^{0.5}$)
	Mercury accessible	Water accessible			
LM–R	32.90 ± 1.87	36.06 ± 1.33	−1.45	0.054	483.1
BaM-10	32.79 ± 1.75	37.12 ± 1.63	−1.54	0.062	595.1
BaM-25	36.40 ± 1.05	37.21 ± 1.55	−1.66	0.065	527.5

Measurements were carried out in triplicate ($n = 3$).

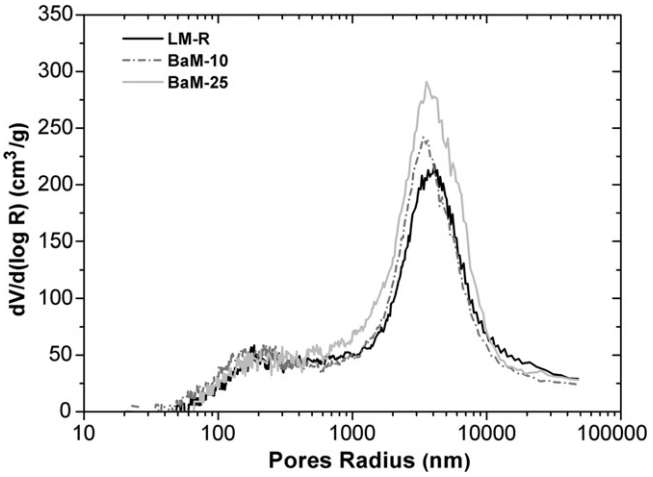

Fig. 2. Differential pore-size distribution for mixtures studied by mercury intrusion porosimetry.

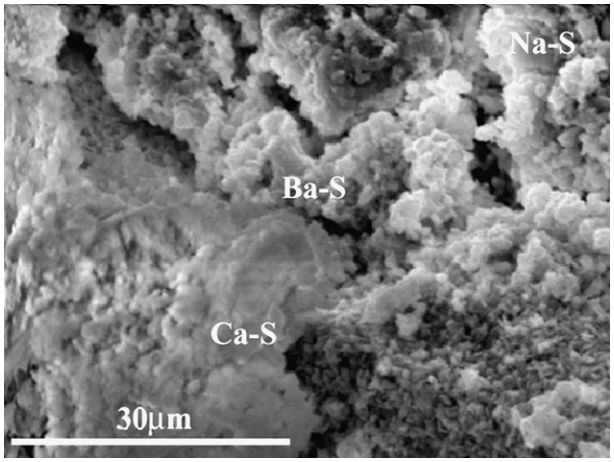

Fig. 4. SEM photomicrograph of a freshly fractured surface from mixture BaM-25 after failure at the 10th cycle. Calcium sulphate (C–S) and barium sulphate (Ba–S) crystals are filling the pores of the specimen, along with the precipitated sodium sulphate crystals.

precipitated within the pores was based on the interpretation of X-ray element mappings, EDX spot analysis and XRD results. Calcite, bassanite ($CaSO_4 \cdot 0.5H_2O$), calcium sulphate hydrate ($CaSO_4 \cdot H_2O$) and thenardite (Na_2SO_4) were the main phases identified. Barite ($BaSO_4$) was identified in all barium mixtures.

Examination of samples under the SEM/EDX revealed that the performance of mixtures is strongly related to the chemistry of their binder. When the reference lime-mixtures are immersed in a sodium sulphate solution the pores of the specimens become impregnated with the salt solution. The pore solution is gradually saturated in respect to thenardite (Na_2SO_4, $K_{sp} = 0.605$) and portlandite [$Ca(OH)_2$, $K_{sp} = 5.02.10^{-6}$], which is derived from the partial dissolution of the non-carbonated lime binder. As the solution approaches saturation with respect to thenardite, at ambient conditions, it becomes supersaturated with respect to mirabilite ($Na_2SO_4 \cdot 10H_2O$) and various phases of calcium sulphate hydrate (Fig. 3). In the presence of a considerable amount of calcium ions, the precipitation of mirabilite is followed by that of ($CaSO_4 \cdot Na_2SO_4$) [34]. As the aging cycles proceed, the concentration and the crystal size of salts, inside the pores increase, leading to the initiation of micro-cracks and the eventual failure of the specimens. Consequently, the actual damage to the lime-mixtures is mainly controlled by the amount of free calcium hydroxide and the crystallization pressure exerted by mirabilite.

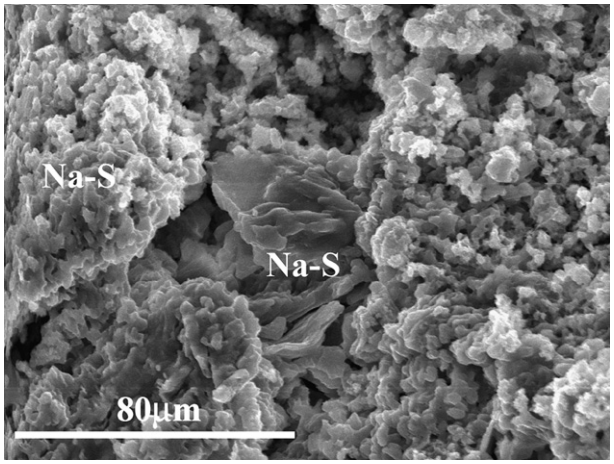

Fig. 3. SEM photomicrograph of a freshly fractured surface from mixture LM–R after failure (7th cycle). Sodium sulphate crystals (Na–S) fill all the available space inside the mortar mass.

In the case of the barium-mixtures (Fig. 4), some of the sulphate ions are fixed by barium and precipitate as barite ($BaSO_4$, $K_{sp} = 1.08.10^{-10}$) on the surface of the pore network and the barium–calcium carbonate solid solution areas. The precipitated barite gradually blocks the further dissolution of Ca^{2+} from the non-carbonated lime binder and, consequently, causes a delay to the precipitation of mirabilite.

3.4. Sulphuric acid attack

The degradation of the mortar mixtures is mainly described by the surface reactions between the sulphuric acid solution and the binding material of the mixtures, such as acid attack, dissolution and leaching of the binding medium (carbonated lime). The development of the above processes also incorporates microstructure parameters such as porosity, diffusion and permeability.

During the acid rain simulation test, the acidic solution flows over the surface of the specimens, reacts with the carbonated lime (Eq. (1)), removes the dissolved Ca^{2+} ions and, therefore, weakens the binding material. However, part of the solution is absorbed by the specimens and fills the pore-space of a surface layer, whilst the remainder runs off. X-ray mapping (SEM/EDX) of sulphur (S) in cross-sectioned surfaces of the specimens at the end of the 20th cycle showed that the thickness of the sulphated layer ranges between 150 and 600 μm. The sulphuric acid absorbed into the pores readily reacts with calcite (Eq. (2)) and gypsum crystals are formed through precipitation. The precipitation of gypsum in the pore solution is also supported by the fixation of Ca^{2+}, which are derived from the dissolution of the non-carbonated lime [24] in the acidic solution. During the next aging cycle the gypsum previously formed dissolves in the acid solution that flows over the surface of specimens and the dissolved ions are removed by the run-off solution. Consequently, the cementing material is weakened and the specimens are degraded.

$$HSO^-_{4(aq)} + CaCO_{3(s)} \rightarrow Ca^{2+}_{(aq)} + SO^{2-}_{4(aq)} + CO_{2(aq)} \quad (1)$$

$$HSO^-_{4(aq)} + SO^{2-}_{4(aq)} + CaCO_{3(s)} \rightarrow CaSO_4 \cdot 2H_2O_{(s)} + CO_{2(aq)} \quad (2)$$

When witherite ($BaCO_3$) participates in the cementing material, its reaction with sulphuric acid leads to the precipitation of barite ($BaSO_4$) (Eq. (3)). Barite has a very low solubility product

(K_{sp} = 1.08.10^{-10}) and is considered practically insoluble. Therefore the release of Ba^{2+} to the run-off solution by the dissolution of witherite (Eq. (4)) does not take place to any significant extent. Considering that during the setting process of barium mixtures a solid solution of barium carbonate in calcium carbonate is formed around calcitic aggregates [24], the formation of barite in those areas consolidates the aggregates in the binding material and therefore increases their resistance against chemical degradation.

$$HSO^-_{4(aq)} + SO^{2-}_{4(aq)} + BaCO_{3(s)} \rightarrow BaSO_{4(s)} + CO_{2(aq)} \quad (3)$$

$$HSO^-_{4(aq)} + BaCO_{3(s)} \rightarrow Ba^{2+}_{(aq)} + SO^{2-}_{4(aq)} \quad (4)$$

The concentration of Ca dissolved and leached from the mixtures was determined by inductively coupled plasma-atomic emission spectroscopy (ICP-AES) and the results were expressed in moles of calcium in 1 l of the run off solution (M). Mixture LM–R showed the highest accumulative concentration of Ca in the run-off solution (8.14.10^{-3} moles/l), followed, in decreasing order, by BaM-10 (7.23.10^{-3} moles/l). In contrast, mixture BaM-25, which contained the maximum amount of barium hydroxide, showed the lowest concentrations (6.50.10^{-3} moles/l). The concentration of barium (Ba) in BaM mixtures was below 5.12.10^{-5} moles/l which, compared to the concentration of Ca, is negligible.

The plot of Ca concentrations in the run-off solutions at different cycles (Fig. 5) shows that the amount of Ca leached from the mixtures decreases with increasing $Ba(OH)_2$. Fig. 5 shows that while the reference mixture (LM–R) gives an almost constant rate of Ca leaching over the testing period, the amount of Ca leached from the barium-mixtures gradually decreases. In the initial stages of the test, the run-off from the barium-mixtures show a much higher Ca concentration than the reference mixture (Fig. 5). This is attributed to the elevated water absorption coefficients (14.8% and 16.6%, respectively) measured in the barium-mixtures and, therefore, to the increased amount of acid solution initially involved in the decay process. After 20 aging cycles, however, the amount of Ca leached from the reference mixture was found to be 56% higher than the BaM-25 mixture. The above phenomenon indicates the development of a protective mechanism, which increases the resistance of barium-mixtures against the leaching of the calcitic binder.

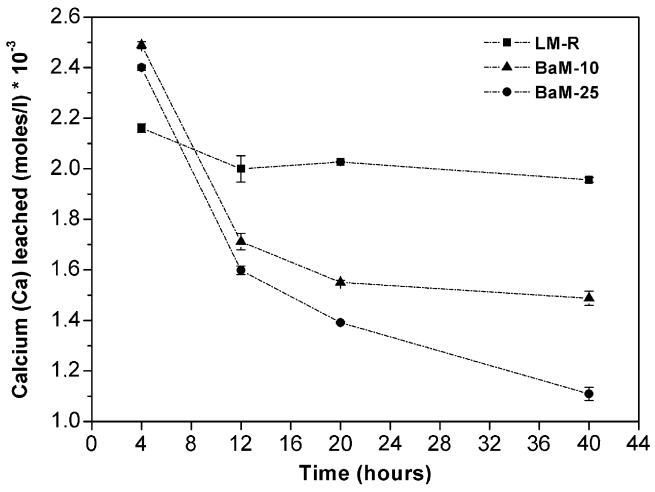

Fig. 5. Concentration of calcium (moles/l) leached form the LM mixtures during the acid rain simulation test.

The examination of fractured surfaces from the external layers of the acid-degraded specimens under the SEM/EDX strengthened the above assumption and provided further information about the morphology and depth of the weathering layers. After 20 aging cycles, the depth of the altered layer of the BaM-25 specimens, containing 25% barium hydroxide, ranged from 100 to 150 μm. For the same period, the altered layer of the reference mixtures (LM–R) ranged from 400 to 600 μm (Fig. 6). The loss of signal in X-ray maps is attributed to the rough morphology (cavities) of the fractured surfaces close to the altered area. The differences in the depth of the sulphated areas are attributed to the amount of barium participating in the mixtures.

Further examination of the altered areas under SEM showed an increased concentration of barium sulphate conglomerates, which precipitate at the interface between the non-altered mortar mass and the gypsum layer (Fig. 7). The precipitation and conglomeration of barium sulphate forms a type of barrier layer, which should be associated with the reduced dissolution rate of the calcitic binder in the lime–barium mixtures (Fig. 5). Thus, the depth of the sulphated layer in the mortars with barium hydroxide gradually reduces to 60% of that formed in the reference mixture (Fig. 6).

Finally, the diffraction patterns of solid material filtered from the acid solution showed that gypsum ($CaSO_4 \cdot 2H_2O$) and small amounts of barite ($BaSO_4$) were the only phases identified.

The interpretation of the above results with the physical properties of the mixtures shows that even if the water absorption coefficients for mixtures BaM-10 and BaM-25 have been slightly increased, the amount of Ca^{2+} leached, and the depth of the sulphated area, presented considerable lower values. This observation supports the assumption that the degradation of the above mixtures depends more on the chemistry of the binding material than the physical properties (pore-space properties) of the mixture.

For the needs of the present study, barium hydroxide was added to lime mortars as a pure chemical product and the overall results proved that the mixtures have the potential to be applied successfully on built heritage and architectural monuments. In field applications it could be used in the same form, since it is commercially available in bulk quantities at prices in between those of hydrated and hydraulic lime. Any additional cost resulted from this choice is not prohibitive for their application, since it is strongly expected to

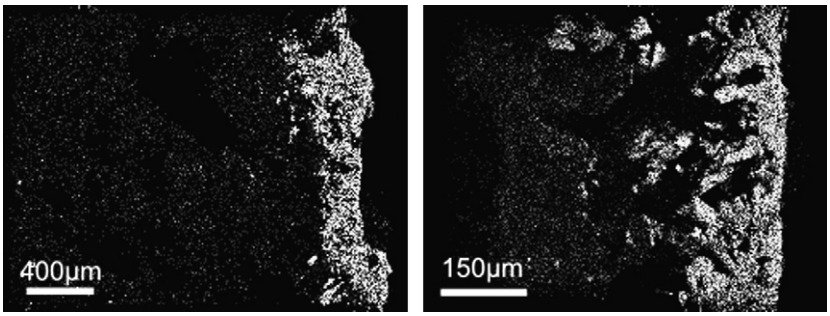

Fig. 6. X-ray maps of S in mixtures LM–R (left) and BaM-25 (right). The depth of the sulphated layer in mixture BaM-25 is approximately half of the one formed in LM–R.

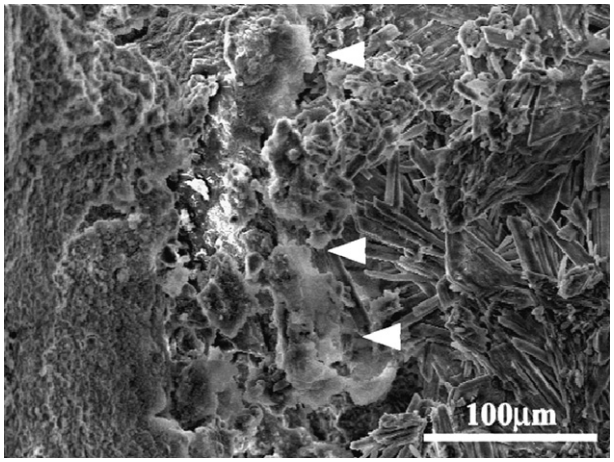

Fig. 7. SEM photomicrograph of mixture BaM-25 after the acid rain simulation test. The layer of ($BaSO_4$), indicated with arrows, lies between the altered and the non-affected mass (within the 200 μm), and acts as a barrier, preventing further attack of the mortar body.

be eliminated through time, due to the superior performance of the barium-mortars, their prolonged service life and the reduced requirements for restoration interventions in sort-time periods.

4. Conclusions

The order of failure for mixtures during the crystallisation tests showed a better performance of the barium mixtures (BaM-10, BaM-25). Their enhanced durability against crystallisation of sodium sulphate was supported by the partial fixation of sulphate through the formation of insoluble barium sulphate. Therefore, the deterioration action of hydrous sodium sulphate salts, through their volume expansion, was partially eliminated.

The crystallisation tests have also shown that the durability of mortars towards the soluble salts is dependent upon the chemistry of their binder (carbonation stage and chemical stability of setting products) and their pore-space characteristics.

In the acid rain simulation test, it was found that the total amount of calcium leached from the mixtures was gradually reduced over time by increasing the amount of barium hydroxide in the mortar. The protective role of the barium compounds can be described by the precipitation of barium sulphate at the interface of the non-altered mass, which forms a barrier layer against further dissolution of the calcitic binder. Thus, the depth of the sulphated layer in the mixture that contained 25% of barium hydroxide in its binder (BaM-25) was reduced to 60% of that formed in the reference mixture (LM–R). The formation of the $BaSO_4$ protecting layer starts as soon as the acid attack takes place and, thus, can be effective from the initial stage of the degradation process. The protective role of barium, therefore, has a direct effect on the service-life of the mortar mixtures.

The results of this work show that the durability of mortars against sulphate depends primarily upon the chemical composition of their binder. In this context, barium hydroxide was found to have a positive effect on the performance of lime-based restoration mixtures, as it increases their durability against sulphate attack without affecting the microstructure and pore-space characteristics of hardened mixtures.

Acknowledgements

The authors would like to acknowledge the collaboration of the following colleagues: Dr. Christos Trapalis at the Institute of Materials Science NCSR Demokritos, for running ICP analysis as well as Dr. Nicos Kanellopoulos and Dr. Andreas Sapalidis at the Institute of Physical Chemistry, NCSR Demokritos, for the Mercury Porosimetry measurements.

References

[1] Yates T. Mechanisms of air pollution damage to brick concrete and mortar. In: Brimblecombe P, editor. Air pollution reviews: the effects of air pollution on the built environment. London: Imperial College Press; 2003. p. 107–32.
[2] Sabbioni C, Zappia G, Riontino C, Blanco-Varela MT, Aguilera J, Puertas F, et al. Atmospheric deterioration of ancient and modern hydraulic mortars. Atmos Environ 2001;35(3):539–48.
[3] Zappia G, Sabbioni C, Pauri MG, Gobbi G. Mortar damage to airborne sulfur compounds in a simulation chamber. Mater Struct 1994;27(8):469–73.
[4] Martinez Ramirez S, Puertas F, Blanco-Varela MT, Thompson GE. Studies on degradation of lime mortars in atmospheric simulation chambers. Cement Concrete Res 1997;27(5):777–84.
[5] Bartos P, Groot C, Hughes JJ, editors. Historic mortars: characteristics and tests. Proceedings of RILEM workshop, Paisley, Scotland. RILEM Publications S.A.R.L.; 1999.
[6] Van Balen K, Toumbakari EE, Blanco-Varela MT, Aguilera J, Puertas F, Palomo A, et al., editors. Environmental deterioration of ancient and modern hydraulic mortar. Research Report No 15, EUR 19863. European Commission, Luxemburg: Office for Official Publications of the European Communities; 2002.
[7] Rendell F, Jauberthie UR. The deterioration of mortar in sulphate environments. Constr Build Mater 1999;13(6):321–7.
[8] Bartos P, Groot C, Hughes JJ, editors. Historic mortars: characteristics and tests. Proceedings of the international RILEM workshop. Paisley: RILEM Publications S.A.R.L.; 2005.
[9] Santhanam M, Cohen MD, Olek J. Mechanism of sulfate attack: a fresh look. Part 2. Proposed mechanisms. Cement Concrete Res 2003;33(3):341–6.
[10] Zappia G, Sabbioni C, Pauri MG, Gobbi G. Mortar damage due to airborne sulfur compounds in a simulation chamber. Mater Struct 1994;27(8):469–73.
[11] Booth J, Hong Q, Compton RG, Prout K, Payne RM. Gypsum overgrowths passivate calcite to acid attack. J Colloid Interf Sci 1997;192(1):207–14.
[12] Wilkins SJ, Compton RG, Viles HA. The effect of surface pretreatment with polymaleic acid, phosphoric acid, or oxalic acid on the dissolution kinetics of calcium carbonate in aqueous acid. J Colloid Interf Sci 2001;242(2):378–85.
[13] Aguilera J, Martınez-Ramırez S, Pajares-Colomo I, Blanco-Varela MT. Formation of thaumasite in carbonated mortars. Cement Concrete Comp 2003;25(8):991–6.
[14] Corinaldesi V, Moriconi G, Tittarelli V. Thaumasite: evidence of incorrect intervention in masonry restoration. Cement Concrete Comp 2003;25(8):1157–60.
[15] van Hees RPJ, Wijffels TJ, van der Klugt LJAR. Thaumasite swelling in historic mortars: field observations and laboratory research. Cement Concrete Comp 2003;25(8):1165–71.
[16] Blanco-Varela MT, Aguilera J, Martinez-Ramiúrez S, Puertas F, Palomo A, Sabbioni C , et al. Thaumasite formation due to atmospheric SO_2–hydraulic mortar interaction. Cement Concrete Comp 2003;25(8):983–90.
[17] Sideris KK, Savva AE, Papayianni J. Sulfate resistance and carbonation of plain and blended cements. Cement Concrete Compos 2006;28(1):47–56.
[18] Mehta PK. Sulfate attack on concrete – a critical review. In: Skalny J, editor. Mater Sci Concrete, vol. III. Westerville: American Ceramic Society; 1992. p. 105–30.
[19] Irassar EF, Bonavetti VL, Gonzalez M. Microstructural study of sulfate attack on ordinary and limestone Portland cements at ambient temperature. Cement Concrete Res 2003;33(1):31–41.
[20] Tikalsky PJ, Carrasquillo RL. Influence of fly ash on the sulphate resistance of concrete. ACI Mater J 1992;89(1):69–75.
[21] Mehta PK. Studies on blended Portland cements containing santorinian earth. Cement Concrete Res 1981;11(4):507–18.
[22] Al-Amoudi OSB. Mechanisms of sulfate attack in plain and blended cements: a review. In: Dhir RK, Hewlett PC, editors. Proceedings of the international congress creating with concrete. Dundee: American Society of Civil Engineers, Thomas Telford Ltd.; 1999. p. 247–60.
[23] Wild S, Knatib JM, O'Farrell M. Sulphate resistance of mortar containing ground brick clay calcined at different temperatures. Cement Concrete Res 1997;27(5):697–709.
[24] Karatasios I, Kilikoglou V, Colston B, Theoulakis P, Watt D. Setting process of lime-based conservation mortars with barium hydroxide. Cement Concrete Res 2007;37(6):886–93.
[25] BS EN 196. Methods of testing cement – Part 1: determination of strength. British Standard Institution; 1995.
[26] Meng B. Characterization of pore structure for the interpretation of moisture transport. In: Thiel MJ, editor. Conservation of stone and other materials. Paris: E&FN Spon; 1993. p. 155–62.
[27] Quenard DA, Xu K, Kunzel HM, Bentz DP, Martys NS. Microstructure and transport properties of porous building materials. Mater Struct 1998;31(5):317–24.
[28] BS EN 1015. Methods of test for mortar for masonry – Part 18: determination of water absorption coefficient due to capillary action of hardened mortar. British Standard Institution; 2002.

[29] BS EN 1925. Natural stone test methods – determination of water absorption coefficient by capillarity. British Standard Institution; 1999.
[30] BS EN 1015. Standard methods of test for mortar for masonry – Part 19: determination of water vapour permeability of hardened rendering and plastering mortars. British Standard Institution; 1999.
[31] BS EN 1936. Natural stone test methods – determination of real density and apparent density, and of total and open porosity. British Standard Institution; 1999.
[32] BS EN 12370. Natural stone test methods – determination of resistance to salt crystallization. British Standard Institution; 1999.
[33] Martinez-Ramirez S, Thompson GE. Wet deposition studies of hydraulic mortars. Mater Struct 1999;32(222):606–10.
[34] Reeves NJ, Clegg SL, Brimblecombe P. Data evaluation and molality-based parameterisation. In: Price C, editor. An expert chemical model for determining the environmental conditions needed to prevent salt damage in porous materials. London: Archetype Publications; 2000. p. 65–116.